Japanese Journal of Applied Physics **57**, 110304 (2018)
https://doi.org/10.7567/JJAP.57.110304

RAPID COMMUNICATION

Spin splitting in EuO(111)/Si(111) spin-filter tunnel junctions with atomically sharp interface

Rento Ohsugi[1]*, Hiroo Omi[1,2], Yoshiharu Krockenberger[1], and Akira Fujiwara[1]

[1]*NTT Basic Research Laboratories, NTT Corporation, Atsugi, Kanagawa 243-0198, Japan*
[2]*NTT Nano Photonics Center, NTT Corporation, Atsugi, Kanagawa 243-0198, Japan*

*E-mail: osugi.rento@lab.ntt.co.jp

Received August 8, 2018; accepted September 18, 2018; published online October 16, 2018

We demonstrate the tunneling in spin-split barriers made of ferromagnetic EuO grown on Si(111) substrates by molecular beam epitaxy. For 6 nm thick EuO films with high crystal quality and atomically sharp interfaces, we find a barrier height lowering driven by the spin splitting below the Curie temperature of 35 K. We determined the splitting energy to be 0.56 ± 0.03 eV at 20 K which results in a spin polarization above 90%.

The development of next-generation electronic devices[1,2] demands for ways and means to generate spin polarized states in Si, e.g., spin metal–oxide–semiconductor field-effect-transistors (spin-MOSFETs[3]). An effective way of generating spin polarized states is the use of the spin filtering effect in ferromagnetic insulators (FMI). These materials have spin-split barrier heights ($\phi_\uparrow$ and $\phi_\downarrow$)[4] where down-spin states tunnel through a barrier higher than that of up-spin states. This leads to a considerable difference of up- and down-spin transmittances due to the exponential dependence of the tunneling probability on the barrier heights. As a result, the tunneling barrier with a large spin-splitting energy effectively polarizes up- and down-spin states.

EuO is known to show large (97%) spin polarizations (P) in FMI/metal junctions,[5–7] and more importantly, it can be grown epitaxially on Si without impeding the Si surface. EuO crystallizes in a simple rock-salt cubic crystal structure [$Fm\bar{3}m$; space group (S.G.), No. 225, $a = 5.144$ Å[8]] and therefore a well matched material with Si ($Fd\bar{3}m$; S.G., No. 227, $a = 5.431$ Å). Thus, the EuO/Si junction has great potential as an ideal spin filter for Si spintronics compared to previously reported Fe/MgO/Si junctions giving $P = 53\%$.[9] To realize high P, the formation of the EuO/Si structure with a high crystalline quality and a sharp interface is crucial for the undistorted transport of spins through the structure.[10,11]

One of the difficulties in forming EuO/Si junctions is known to be related to the Eu–O_2–Si thermodynamics.[12,13] The precise control of the oxygen pressure during the growth of EuO on Si is inevitable[14] to avoid the formation of antiferromagnetic Eu_3O_4[15] and paramagnetic Eu_2O_3.[16] Moreover, Eu-silicides[17] and Eu-silicates[18] are likely formed at EuO/Si interfaces. It has been found that such intermixing effects can be suppressed by the growth of EuO on adatom-terminated Si surfaces.[14,17] Recently, epitaxial growth of EuO has been reported with Eu-terminated Si(100)-(5×1)[17] and Eu-terminated Si(111)-(2×1)[19] to which a surface structure model has been proposed.[20] However, there has been no experimental demonstration of spin filtering of EuO/Si junctions, suggesting that the quality of the EuO thin films and interfaces are still insufficient.

In this letter, we present a systematic study of the epitaxial growth of EuO on Si with a variety of Eu-terminations on Si(111). Here, special care has been taken to assure atomically sharp interfaces between EuO and Si. To evaluate the spin filtering of EuO/Si junctions, we fabricated tunnel junction devices. These devices exhibit a clear temperature dependence of the tunnel current through ferromagnetic EuO epitaxially grown on Si.

These EuO thin films were grown by reactive molecular beam epitaxy (MBE[21]). As an oxidizing agent, we used molecular O_2 supplied by a nozzle located 15 cm below the Si substrate. We used Eu metal and evaporated from a Knudsen cell at cell temperature of 500 °C [Eu flux 5.3×10^{14} atoms/(cm^2·min)]. Si(111) substrates were prepared by a wet chemical process[22] prior to installing them in the MBE chamber. For Si surfaces, it is known that a 7×7-Si reconstructed surface ensures wide ranging atomical flatness.[23] Therefore, prior to the growth, we ensured the existence of such a 7×7-Si surface by reflection high-energy electron diffraction (RHEED) while heating the substrate to a temperature of $T_S = 760$ °C under vacuum (1.8×10^{-10} Torr). We deposited a thin Eu-termination layer on the Si(111) surface at $T_S = 720$ °C. Then, we decreased T_S to 510 °C, and subsequently supplied O_2 at a pressure of 8.0×10^{-9} Torr, corresponding to a flux of 4.8×10^{13} O_2 molecules/(cm^2·min). Eu atoms and O_2 molecules were simultaneously supplied during the growth of the EuO layers. After the growth of EuO films, the T_S was rapidly lowered to room temperature.

The cubic crystal structure of the EuO films was identified by X-ray diffraction (XRD). Figure 1(a) shows a typical example of the XRD profile from the film grown on a 2×1 Eu-terminated Si(111). The observed diffraction peaks coincide with EuO(111), (222), and (333) peaks, respectively,[8] and there are no indications of other impurity phases. These peaks prove that the EuO films are (111)-oriented, parallel to the (111) axis of Si. By analyzing the position of these peaks, a cubic lattice constant of the EuO thin films was calculated by the Nelson–Riley method[24] to be $a = 5.24 \pm 0.05$ Å. This lattice constant is slightly larger than that of bulk EuO ($a = 5.144$ Å[8]), suggesting that the EuO films are strained along the ⟨111⟩ direction with a tensile strain of 1.89%.

The growth of EuO films can be influenced by the degree of Eu-termination on Si. We evaluated the EuO(222) diffraction intensities for different Eu-terminations [Fig. 1(b)]. It was found that the 2×1 Eu-termination with a thickness of 1.87 ± 0.10 Å resulted in the highest XRD peak intensity. The other terminations, e.g., 7×1 and 3×1 resulted in significantly lower XRD intensity. This is also true if the Eu-termination is absent. These results clearly indicate that the crystalline quality of EuO strongly depends on the surface termination schemes and it is the best with the 2×1 Eu-

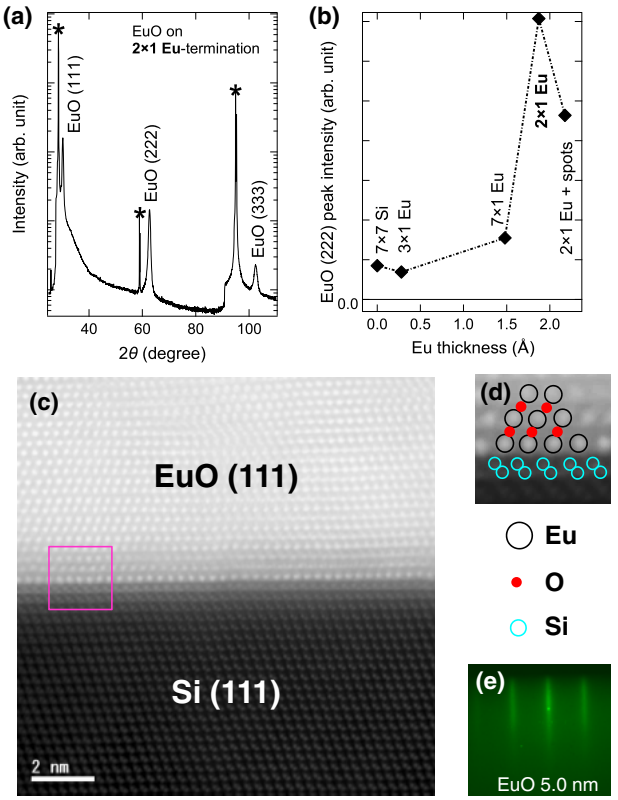

Fig. 1. (Color online) (a) The XRD profile of the 28.2 nm thick EuO film grown on a Si(111) substrate with a Eu-termination of 1.87 Å. Diffraction peaks of the Si substrate are marked with asterisks. (b) EuO(222) diffraction peak intensities as a function of the effective thicknesses of the Eu-termination layers. The Eu layer thickness was determined by the quartz crystal micro balance. The EuO thicknesses were constant at 28.2 nm. Data points are labelled by the surface reconstruction matrix prior to the EuO growth. The surface reconstructions are determined by RHEED measurements (not shown). (c) is cross sectional STEM image of a EuO/Si(111) structure. The accelerating voltage was 200 kV. All cross-sections are along {110} planes. (d) is enlarged image of the boxed region in (c). The black, red, and blue circles are showing the positions of Eu, O, and Si atoms, respectively. As the positions of the lightweight O^{2-} ion are invisible, we assumed them from the relative position of Eu^{2+} ions. (e) is the RHEED pattern taken from the surface of a 5 nm thick EuO film. The incidental direction of the electron beam was fixed to $[1\bar{1}0]$.

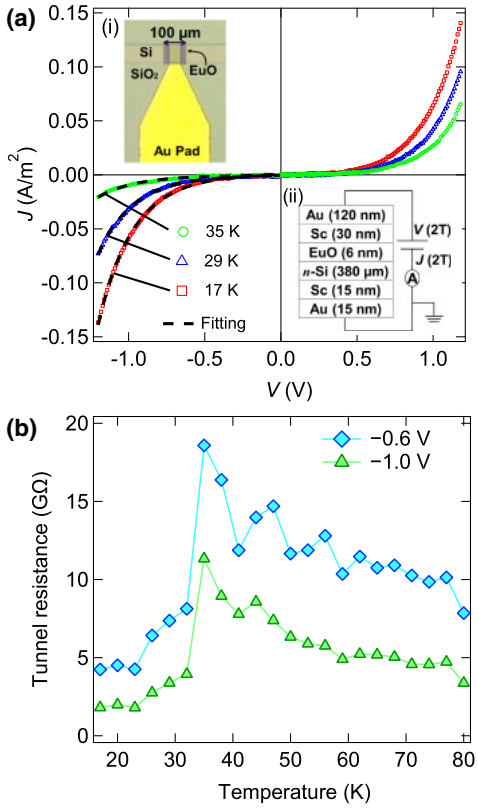

Fig. 2. (Color online) (a) Temperature dependence of *J*–*V* curves taken from the EuO/Si junction with EuO thickness of 6 nm. The dashed lines shows fitting curves by Simmons model. A microscope image from top view of the junction is exhibited in the inset (i). The inset (ii) schematically shows the layer structure and the measurement configuration of the device. (b) Temperature dependence of the junction resistances taken at applied bias voltages of −0.6 and −1.0 V in the *J*–*V* curves.

termination, which is a surface structure that allows for complete coverage of the Si surface.[20] Therefore, the formation of a 2×1 Eu-termination layer suppresses Eu–O–Si ternary reactions. On the other hand, a thicker Eu-termination (>2 Å) results in the formation of islands of Eu-silicides,[17] thus degrading the interface crystalline quality.

Next, we characterized the EuO/Si interface by cross-sectional scanning transmission electron microscopy (STEM). The STEM image in Fig. 1(c) shows that the epitaxial film is composed of single phase EuO. First of all, the interface area between EuO and Si is abrupt. Moreover, the STEM image shows a contrast variation in the vicinity of the interface. We therefore analyzed the interface region by energy dispersive X-ray analysis and found an oxygen concentration higher than what is expected for stoichiometric EuO. The interface area is further magnified in Fig. 1(d) to highlight the atomic configurations of the interface formed by EuO growth on the 2×1 Eu-terminated Si surface. One can recognize that the Eu ions are located on the silicon atoms with a lateral Eu–Eu distance ∼3.21 Å, indicating that the EuO(111) ‖ Si(111) and EuO⟨110⟩ ‖ Si⟨110⟩ alignments originate from the interface. Moreover, no intermixing layer is discernible, emphasizing the atomically sharp interface between EuO and Si. Furthermore, as shown in Fig. 1(e), to ensure a uniform growth of EuO, we monitored the growth in real-time by RHEED. In Fig. 1(e), we show a RHEED image taken after growth of a 5 nm thick EuO film. The streak pattern indicates atomically flat surface of the EuO film has formed, which is in contrast to the spotty RHEED pattern in the previous study.[19] This strongly suggests that EuO was grown uniformly in our sample, which will be important for the fabrication of tunnel junction devices with thin ferromagnetic EuO barriers.

The spin polarized tunneling current ($J_\uparrow$ or $J_\downarrow$) through such device contains the information related to the barrier heights as well as the degree of *P*. We fabricated metal/EuO/Si tunnel junctions with a different areas *S* ($S = 0.64$, 1.00, 2.25×10^{-2} mm^2) by using patterned Au/Sc as contact metal on EuO and Si. The Si substrate used here is n-type (P doped) with a doping density of $\sim 10^{16}$/cm^2. The layer structure [inset (ii) in Fig. 2(a)] is Au (120 nm)/Sc (30 nm)/EuO (6 nm)/Si (380 μm)/Sc (15 nm)/Au (15 nm). Note that we selected Sc as a contact material because Sc ensures Ohmic contact with Si and good adhesion with EuO. The devices were mounted on a cooling stage in a probe station to measure the temperature dependence of the current density–voltage (*J*–*V*) curves. *J*–*V* measurements were performed by

a two terminal configuration with a source measure unit (Keithley 2635B). As the series resistances (~500 Ω) of the Sc/Si interface and the Si substrate were smaller by eight orders of magnitude compared to the EuO tunnel tunnel resistance. It is safe to assume that the voltage drop measured occurs only at the EuO tunnel barrier. We varied the sample temperature from 17 to 80 K while simultaneously acquiring J–V data. We determined the spin splitting of the barrier heights and T_C of EuO barriers by investigating the temperature dependence of tunnel resistance at zero magnetic field. This method is commonly used to determine spin splitting barrier heights of FMI/metal junctions as shown in previous studies,[6,7] where spin splitting was detected as abrupt resistance change below T_C and the splitting energy could be extracted by means of fittings of J–V curves with proper tunnel current models. Here, we focused on the J–V measurements of 6 nm thick EuO films as EuO films with a thickness of 3 nm did not show the spin splitting whereas the resistance for larger thicknesses exceeded our measurement range.

Figure 2(a) shows the J–V curves of the device with $S = 1.00 \times 10^{-2}$ mm^2 at three different temperatures, i.e., 17, 29, and 35 K. The current densities exhibit a nonlinear increase with bias voltage. This indicates that the EuO (6 nm) acts as a tunnel barrier and the tunnel probability is bias dependent. Such a bias dependency can be analyzed by Simmons model.[25] What is striking in Fig. 2(a) is that the tunnel current significantly increases as the temperature decreases, which cannot be explained by normal tunnel barriers and strongly suggests that the barrier height rapidly change as the temperature varies. Note that, a similar temperature dependence was reproduced for devices independent of S. As the J–V response is independent of S, it supports that the observed behavior is intrinsic nature of EuO barrier.

Using the J–V data, we determine the tunnel resistances and plotted it as a function of temperature for two different bias voltages in Fig. 2(b). Independent of the bias voltage, the resistance monotonically increases above 35 K and suddenly drops by 1/5 below 35 K. The abrupt reduction of the resistances is associated to the reduced tunnel barrier heights of ferromagnetic EuO below T_C.[6,7] Below T_C, the conduction-band bottom of the barrier splits into two spin-dependent levels (up- and down-spin)[4] with a splitting energy $2\Delta E$ as shown in Fig. 3(b) later. The spin-split barrier heights relating to the ΔE are defined as $\phi_\uparrow = \phi(T_C) - \Delta E$ and $\phi_\downarrow = \phi(T_C) + \Delta E$. Here, the $2\Delta E$ changes proportionally to the magnetization M as $\Delta E(T) \propto M(T)/M(T=0)$.[6] Therefore, the $\Delta E(T)$ becomes smaller with increasing temperatures, and it is zero above T_C, and therefore, $\phi_\uparrow(T) = \phi_\downarrow(T)$ in the paramagnetic state of EuO. The T_C of the ferromagnetic layer embedded in the spintronic device [inset (i) in Fig. 2(a)] was $T_C = 35$ K, which is lower than that of bulk EuO (69 K)[26] and the 40 nm thick EuO film (68 K) of the previous study.[19] As it is previously reported that oxygen-rich EuO films drastically reduce T_C to be less than 15 K,[27,28] consequently, the oxygen-rich layer [see Fig. 1(c)] occupying a volume of 20% in our thin EuO films, can cause a reduction of T_C.

Next, we analyzed the spin-dependent barrier heights to estimate efficiency of spin filtering driven by the spin splitting $2\Delta E$. This requires an estimation of the barrier heights which we determine from J–V curves using Simmons

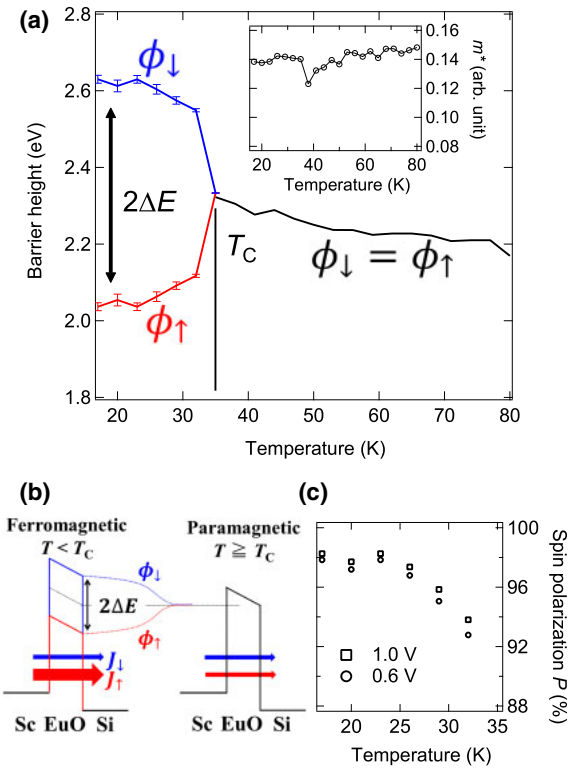

Fig. 3. (Color online) (a) Temperature dependence of tunneling barrier heights determined by the fittings of J–V curves in Fig. 2(a). The red and blue lines show the barrier heights for up- and down-spins, respectively. Above T_C, the tunneling barrier heights are spin-independent due to the paramagnetic state of EuO. Inset: the temperature dependence of the effective tunneling mass derived by Simmons model. (b) A sketch of the barrier height lowering due to ferromagnetic transition of EuO. (c) The P values of the tunneling current density under reverse bias voltages of −0.6 V (circle) and −1.0 V (square) below T_C.

tunnel model.[25,29] In Simmons model, the current density J is given as

$$J = J_\uparrow + J_\downarrow$$
$$= \frac{1}{2}\sum_{\sigma=\uparrow,\downarrow} A\left\{\left(\phi_\sigma(\Delta E) - \frac{eV}{2}\right)\exp\left[B\left(\phi_\sigma(\Delta E) - \frac{eV}{2}\right)\right]\right.$$
$$\left. - \left[\phi_\sigma(\Delta E) + \frac{eV}{2}\right)\exp\left[B\left(\phi_\sigma(\Delta E) + \frac{eV}{2}\right)\right]\right\},$$
$$A = \left(\frac{e}{2\pi h d^2}\right), \quad B = -\frac{4\pi d}{h}\sqrt{2m^* m_0},$$

where $J_\uparrow$ and $J_\downarrow$ are the spin-dependent current densities, e is the electron charge, m_0 and m^* are the mass of free electron and the effective tunneling mass, respectively, h is Planck's constant, d is the thickness of the EuO barrier, and V is the applied voltage. Above T_C, for the numerical fitting process, we set $\phi_\uparrow(T) = \phi_\downarrow(T)$ and m^* as fitting parameters. This results in a barrier height of 2.33 eV and $m^* = 0.14$ at T_C. Then, below T_C, we fixed the barrier height $\phi(T_C) = 2.33$ eV, whereas ΔE and m^* are fitting parameters. Moreover, we kept the tunneling parameters A, B constant using a ferromagnetic thickness of $d = 6$ nm. The fitting curves (dashed line) together with the measured data are shown in Fig. 2(a) in the reverse bias region where the spins are injected from EuO into Si, supposing that the device operates as a spin filter of Si. The m^*s determined by this method are $m^* = 0.14 \pm 0.02$, which is smaller than that of bulk Gd:EuO ($m^* = 0.4$),[30] but

comparable to other transition metal oxides e.g., HfO_2 (0.15) and Y_2O_3 (0.25).[31)]

Figure 3(a) shows the temperature dependence of the obtained barrier heights. The barrier heights above T_C are 2.08–2.57 eV. Using the work function of Sc at 3.5 eV, the barrier heights are converted into EuO's electron affinities of 0.93–1.42 eV. Reported values for the EuO electron affinity range between 0.6 to 1.8 eV[32,33)] and our values are in this range. More importantly, it is clearly shown that ΔE grows rapidly below T_C, consistent with the rapid decrease of the tunnel resistance. The splitting energy $2\Delta E$ reaches 0.56 ± 0.03 eV at 20 K, which well coincides with the previously reported value of 0.6 eV obtained from Auger spectroscopy at 20 K.[34)] The large spin splittings in tunneling barrier heights observed here suggest that P might be close to 100%. To evaluate P of our EuO/Si junction, we calculate $P = (J_\uparrow - J_\downarrow)/(J_\uparrow + J_\downarrow)$ and found it to be larger 90%. Influences of spin flip processes due to possible imperfections at the EuO interface are neglected for simplicity. The temperature dependence of P is plotted in Fig. 3(c). Below 32 K, P is larger than 90% [Fig. 3(c)]. At 17 K, the maximum P of $98 \pm 0.5\%$ and this is comparable to the reported P of 97% in the Al/EuO/Y junction.[6)]

In summary, we surveyed the influences of various Eu-terminations on the Si(111) surfaces to improve on the crystalline quality of epitaxially grown EuO thin films. We found that the 2×1 Eu-termination is optimal to form atomically sharp interfaces between Si(111) and EuO(111). Using the high crystalline quality EuO(111) tunnel barrier with the atomically sharp interface, we investigated the temperature dependence of the tunnelling barrier heights of EuO(111) on Si. We observed that, below T_C, the tunneling barrier height is reduced and this corresponds with the spin filtering phenomena. The evaluated spin splitting in the EuO film is 0.56 eV and the estimated spin polarizations are larger than 90%. More work should be done to investigate the electron affinity and the J–V characteristics under magnetic fields.

Acknowledgment Authors thank Dr. Mitate of NTT Advanced Technology Corporation for observing cross-sectional STEM images.

1) R. Jansen, Nat. Mater. **11**, 400 (2012).
2) S. Manipatruni, D. E. Nikonov, and I. A. Young, Nat. Phys. **14**, 338 (2018).
3) S. Sugahara and M. Tanaka, J. Appl. Phys. **97**, 10D503 (2005).
4) J. S. Moodera, T. S. Santos, and T. Nagahama, J. Phys.: Condens. Matter **19**, 165202 (2007).
5) J. S. Moodera, R. Meservey, and X. Hao, Phys. Rev. Lett. **70**, 853 (1993).
6) T. S. Santos, J. S. Moodera, K. V. Raman, E. Negusse, J. Holroyd, J. Dvorak, M. Liberati, Y. U. Idzerda, and E. Arenholz, Phys. Rev. Lett. **101**, 147201 (2008).
7) M. Müller, G. Miao, and J. S. Moodera, Europhys. Lett. **88**, 47006 (2009).
8) H. A. Eick, N. C. Baenziger, and L. Eyring, J. Am. Chem. Soc. **78**, 5147 (1956).
9) A. Spiesser, H. Saito, Y. Fujita, S. Yamada, K. Hamaya, S. Yuasa, and R. Jansen, Phys. Rev. Appl. **8**, 064023 (2017).
10) R. M. Stroud, A. T. Hanbicki, Y. D. Park, G. Kioseoglou, A. G. Petukhov, B. T. Jonker, G. Itskos, and A. Petrou, Phys. Rev. Lett. **89**, 166602 (2002).
11) S. P. Dash, S. Sharma, J. C. Le Breton, J. Peiro, H. Jaffrés, J. M. George, A. Lemaître, and R. Jansen, Phys. Rev. B **84**, 054410 (2011).
12) *Synthesis of Lanthanide and Actinide Compounds*, ed. L. R. Morss and G. Meyer (Springer, Dordrecht, 1991) Topics in f-Element Chemistry, Vol. 2.
13) A. S. Borukhovich and A. V. Troshin, *Europium Monoxide: Semiconductor and Feromagnet for Spintronics* (Springer, Cham, 2018) Springer Series in Materials Science, Vol. 265, Chap. 2.
14) C. Caspers, A. Gloskovskii, M. Gorgoi, C. Besson, M. Luysberg, K. Z. Rushchanskii, M. Ležaić, C. S. Fadley, W. Drube, and M. Müller, Sci. Rep. **6**, 22912 (2016).
15) K. Ahn, V. K. Pecharsky, and K. A. Gschneidner, Jr., J. Appl. Phys. **106**, 043918 (2009).
16) S. M. Watson, T. S. Santos, J. A. Borchers, and J. S. Moodera, J. Appl. Phys. **103**, 07A719 (2008).
17) D. V. Averyanov, C. G. Karateeva, I. A. Karateev, A. M. Tokmachev, A. L. Vasiliev, S. I. Zolotarev, I. A. Likhachev, and V. G. Storchak, Sci. Rep. **6**, 22841 (2016).
18) E. Kaldis, P. Streit, and P. Wachter, J. Phys. Chem. Solids **32**, 159 (1971).
19) D. V. Averyanov, I. S. Sokolov, A. M. Tokmachev, I. A. Karateev, O. A. Kondratev, A. N. Taldenkov, O. E. Parfenov, and V. G. Storchak, J. Magn. Magn. Mater. **459**, 136 (2018).
20) K. Sakamoto, A. Pick, and R. I. G. Uhrberg, Phys. Rev. B **72**, 195342 (2005).
21) T. Tawara, H. Omi, T. Hozumi, R. Kaji, S. Adachi, H. Gotoh, and T. Sogawa, Appl. Phys. Lett. **102**, 241918 (2013).
22) A. Ishizaka and Y. Shiraki, J. Electrochem. Soc. **133**, 666 (1986).
23) H. C. Jeong and E. Williams, Surf. Sci. Rep. **34**, 171 (1999).
24) J. B. Nelson and D. P. Riley, Proc. Phys. Soc. **57**, 160 (1945).
25) J. G. Simmons, J. Appl. Phys. **34**, 2581 (1963).
26) J. Schoenes and P. Wachter, Phys. Rev. B **9**, 3097 (1974).
27) T. Gerber, P. Lömker, B. Zijlstra, C. Besson, D. N. Mueller, W. Zander, J. Schubert, M. Gorgoid, and M. Müller, J. Mater. Chem. C **4**, 1813 (2016).
28) C. Caspers, M. Müller, A. X. Gray, A. M. Kaiser, A. Gloskovskii, C. S. Fadley, W. Drube, and C. M. Schneider, Phys. Rev. B **84**, 205217 (2011).
29) X. Hao, J. S. Moodera, and R. Meservey, Phys. Rev. B **42**, 8235 (1990).
30) R. M. Xavier, Phys. Lett. A **25**, 244 (1967).
31) C. L. Hinkle, C. Fulton, R. J. Nemanich, and G. Lucovsky, Microelectron. Eng. **72**, 257 (2004).
32) D. E. Eastman and M. Kuznietz, J. Appl. Phys. **42**, 1396 (1971).
33) G. Busch, P. Cotti, and P. Munz, Solid State Commun. **7**, 795 (1969).
34) P. G. Steeneken, L. H. Tjeng, I. Elfimov, G. A. Sawatzky, G. Ghiringhelli, N. B. Brookes, and D. J. Huang, Phys. Rev. Lett. **88**, 047201 (2002).